**DOI:** 10.3969/j.issn.1673-3185.2016.05.008 **http:** // english.ship-research.com

**Translated from:** XIAO Qing, XIE Junchao, CHEN Dongyang. Flutter calculation and analysis of rudder system[J]. Chinese Journal of Ship Research, 2016, 11(5): 48-54.

# Flutter calculation and analysis of rudder system

*XIAO Qing*[1], *XIE Junchao*[1], *CHEN Dongyang*[2]

1 China Ship Development and Design Center, Wuhan 430064, China

2 Institute of Launch Dynamics, Nanjing University of Science and Technology, Nanjing 210094, China

**Abstract:** In researching the fluid elastic characteristics of the rudder system, it is found that the results of rudder system flutter characteristics based on the binary linear flutter wing model are consistent compared with the literature simulation data. The rudder system flutter influence laws of such linear parameters as frequency ratio, gravity center and torsional rigidity are obtained by calculating using the aforementioned model. In addition, combined with calculation method of the two degrees of freedom binary wing hydrodynamic for the arbitrary time domain, the rudder system nonlinear flutter phenomenon is calculated, and the influence of nonlinear flutter caused by the transmission interval is analyzed. The research results provide a fundamental analysis method for the fluid elastic characteristics of rudder systems. The results can also support the anti-flutter design of rudder systems.

**Key words:** rudder system; fluid elasticity; flutter; interval; nonlinearity

**CLC number:** U664.36

## 0 Introduction

In common calculations of fluid elasticity, binary wing is a hypothetical rudder blade, a simplified simulation of the true elastic one, and is generally used for principle analysis and verification of aeroelastic or fluid elastic problems[1-3]. Under this assumption, the airfoils in all sections along the spanwise direction are the same, while the rudder blades are assumed to be absolutely rigid. Bending and torsional deformations of the rudder blades are used for the simulation of the heaving and pitching motion of the two degrees of freedom wing, respectively[4-5]. In general, these theories above can be used to estimate the rudder surface's flow stability of the underwater vehicles[6-10]. Based on the aforementioned researches and Theodorsen theory, taking the flutter characteristics of the underware vehicle's rudder system into full account, this study adopts the hydrodynamic calculation method for the two degrees of freedom binary wing in arbitrary time domain to calculate the rudder surface's nonlinear fluid elasticity. Besides, it also is used to investigate the effects of generalized structural nonlinear factors consisting of the link mechanism interval and bearing friction of rudder system as well as the coupling effects between the rudder system and the control system on flutters. This method is easy for engineering fulfillment and can provide an effective way for nonlinear fluid elasticity analysis of the rudder system. Firstly, the linear and nonlinear models of binary flutters should be established, based on which, the calculation and analysis of linear flutters are carried out. Then, the calculation result is supposed to be compared with that in references. After the nonlinear flutters being calculated and analyzed further, influence laws of such system parameters on flutters are obtained.

## 1 Linear and nonlinear calculating models of binary flutters

According to the rudder system model shown in Fig. 1(a), a simplified model of the wing structure is obtained as shown in Fig. 1(b), as well as the simpli-

**Received:** 2015 - 12 - 23

**Author(s):** XIAO Qing (Corresponding author), male, born in 1979, Ph. D., senior engineer. Research interest: marine fittings. E-mail: xqzju98@163.com

XIE Junchao, male, born in 1984, master, engineer. Research interest: marine fittings. E-mail: xiejunchao@126.com

CHEN Dongyang, male, born in 1988, Ph. D. candidate. Research interest: multi-body dynamics. E-mail: cdy_1988@sina.cn

fied models of the linear and nonlinear flutters of the two degrees of freedom wing (Fig. 1(c) and Fig. 1(d)). The wing connects to the structure through the axial bearing, and in the figures: $v$ is the velocity of the wing relative to the water flow, m/s; $b$ is a half of wing's chord length; $x_a$ is the distance from the mass center to the elastic shaft; $\alpha$ is the pitching rotation angle around the stiffness center. The operation of the overall system from the steering engine to the control surface is to provide a torque to the rudder so that it can swing up and down. Therefore, the entire control system is simplified as a torsional spring for calculation. Through three-dimensional geometric software, location of the mass center and moment of inertia of the rudder blade (including the water inside) are obtained. Then through statics analysis, the position of the elastic shaft of the rudder blade can be found, and the equivalent bending rigidity and equivalent torsional rigidity of rudder blade as well as the equivalent torsional spring rigidity of the control system are calculated.

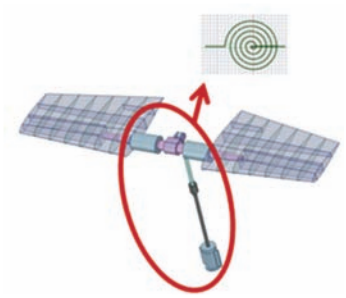

(a) Rudder system model

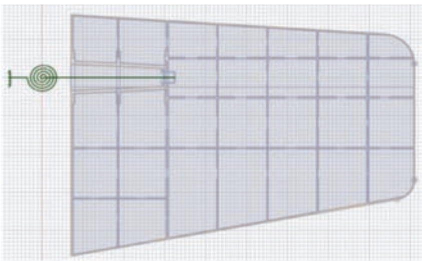

(b) Simplified model of rudder system

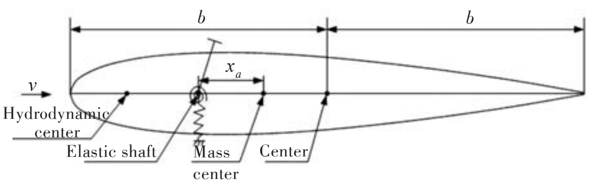


(c) Linear flutter model of two degrees of freedom wing

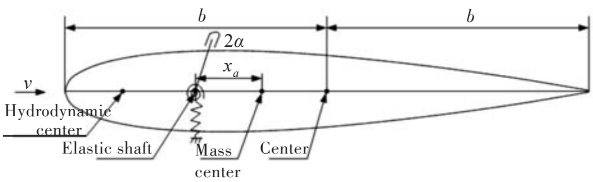


(d) Nonlinear flutter model of two degrees of freedom wing

Fig.1 Simplified model of two binary linear and nonlinear flutter

## 2 Calculation and analysis of linear flutters of binary wing

### 2.1 Calculation model

Differential equations of motion of binary wing's linear flutters are:

$$m\ddot{h} + mx_a\ddot{\alpha} + k_h h = -L(t) \quad (1)$$

$$mx_a\ddot{h} + I_\alpha\ddot{\alpha} + k_\alpha\alpha = T_\alpha(t) \quad (2)$$

where $m$ is the mass of the wing; $k_h$ is the linear spring rigidity; $k_\alpha$ is the torsional spring rigidity; $h$ is the heaving displacement of stiffness center; $I_\alpha$ is the sailplane's moment of inertia to the stiffness center in per unit span; $L$ is the lift; $T_\alpha$ is the pitching moment; and $t$ is time.

The lift $L$ and pitching moment $T_\alpha$ of the binary wing in simple harmonic motion can be written as:

$$L = \pi\rho_a b^2\left[\ddot{h} + v\dot{\alpha} - b\bar{a}\ddot{\alpha}\right] + 2\pi\rho_a vbC(k)\cdot \left[v\alpha + \dot{h} + b\left(\frac{1}{2} - \bar{a}\right)\dot{\alpha}\right] \quad (3)$$

$$T_\alpha = \pi\rho_a b^2\left[b\bar{a}\ddot{h} - vb\left(\frac{1}{2} - \bar{a}\right)\dot{\alpha} - b^2\left(\frac{1}{8} + \bar{a}^2\right)\ddot{\alpha}\right] + 2\pi\rho_a vb^2\left(\bar{a} + \frac{1}{2}\right)C(k)\left[v\alpha + \dot{h} + b\left(\frac{1}{2} - \bar{a}\right)\dot{\alpha}\right] \quad (4)$$

where $\rho_a$ is the fluid density; $C(k)$ is the damping coefficient, and the non-circulation part unrelated to $C(k)$ describes the inertial effect; and $\bar{a}$ is the distance from the elastic shaft to the center.

When $v$ is equal to the flutter velocity $v_g$, the wing is in simple harmonic motion, namely, $h = \bar{h}e^{i\omega t}$, $\alpha = \bar{\alpha}e^{i\omega t}$, where, $\bar{h}$ and $\bar{\alpha}$ are initial displacement and angle respectively. The corresponding hydrodynamic force $F$ and the pitching moment $T_\alpha$ are also in simple harmonic motion, that is: $F = \bar{F}e^{i\omega t}$, $T_\alpha = \bar{T}_\alpha e^{i\omega t}$.

Nondimensionalization is conducted on the simultaneous equation of Eq. (1) and Eq. (2) and then $v-g$ method can be adopted to analyze the flutter. Assuming the structural damping of the rudder system is 0, after the introduction of artificial structural damping, the equation can be rewritten as:

$$\left(\boldsymbol{A}(k) + \boldsymbol{M}\right)\begin{Bmatrix}\bar{h}/b \\ \bar{\alpha}\end{Bmatrix} = \frac{(1 + ig)}{\Omega^2}\boldsymbol{K}\begin{Bmatrix}\bar{h}/b \\ \bar{\alpha}\end{Bmatrix} \quad (5)$$

where,

$$\boldsymbol{M} = \begin{bmatrix}1 & \bar{x}_a \\ \bar{x}_a & \bar{\gamma}_a^2\end{bmatrix}$$

$$\boldsymbol{K} = \begin{bmatrix}R_\omega^2 & 0 \\ 0 & \bar{\gamma}_a^2\end{bmatrix}$$

$$A(k)=$$

$$\frac{1}{\mu}\begin{bmatrix} L_h & L_\alpha-\left(\frac{1}{2}+a\right)L_h \\ \boldsymbol{M}_h-\left(\frac{1}{2}+a\right)L_h & \boldsymbol{M}_\alpha-\left(\frac{1}{2}+a\right)(L_\alpha+\boldsymbol{M}_h)+\left(\frac{1}{2}+a\right)^2 L_h \end{bmatrix}$$

and

$$L_h=1-\mathrm{i}2C(k)\frac{1}{k}$$

$$L_\alpha=\frac{1}{2}-\mathrm{i}\frac{1+2C(k)}{k}-\frac{2C(k)}{k^2}$$

$$\boldsymbol{M}_h=\frac{1}{2}$$

$$\boldsymbol{M}_\alpha=\frac{3}{8}-\mathrm{i}\frac{1}{k}$$

$$\mu=\frac{m}{\pi\rho_a b^2}$$

Let

$$\Omega^2=\omega^2/\omega_\alpha^{\ 2}\ ,\ R_\omega^{\ 2}=\omega_h^{\ 2}/\omega_\alpha^{\ 2}\ ,\ k=\omega b/v$$

where $\bar{\gamma}_a$ is the dimensionless turning radius of the wing around the elastic shaft; $a$ is the dimensionless quantity of the distance from the elastic shaft to the center; $\Omega$ is the ratio of the frequency of simple harmonic motion to natural torsional frequency; $R_\omega$ is the ratio of natural heaving frequency to natural torsional frequency; $\omega$ is the frequency of the wing in simple harmonic motion; $\omega_\alpha$ is the natural torsional frequency of the system; $\omega_h$ is the natural heaving frequency of the system; and $k$ is the reduced frequency.

Then, the eigenvalue of Eq. (5) can be written as

$$\lambda=\frac{(1+\mathrm{i}g)}{\Omega^2}=\lambda_{\mathrm{Re}}+\mathrm{i}\lambda_{\mathrm{Im}} \tag{6}$$

Thus

$$\omega=\frac{\omega_\alpha}{\sqrt{\lambda_{\mathrm{Re}}}}\ ,\ g=\frac{\lambda_{\mathrm{Im}}}{\lambda_{\mathrm{Re}}}\ ,\ v=\frac{\omega_\alpha b}{k\sqrt{\lambda_{\mathrm{Re}}}} \tag{7}$$

When the flutter analysis is done by $v-g$ method, firstly, a certain fluid density $\rho_{\mathrm{a}}$ is given and the values of a set of reduced frequency $k$ are preset; then the complex eigenvalues above are calculated from the maximum $k$, and the corresponding structural damping coefficient $g$, frequency $\omega$ and velocity $v$ are obtained; finally, the values of $g$, $\omega$, $v$ are calculated when $k$ is decreased by a certain step length. The results can be drawn as $v-g$ or $v-\omega$ curve after repeated calculations, and when the calculated $g$ is equal to the true structural damping value $g_0$ of wing, the corresponding $v$ is its critical flutter velocity $v_{\mathrm{F}}$. It should be noted that, the true structural damping coefficient of wing is usually assumed to be 0 during the implementation of the $v-g$ method because it is difficult to be measured; when the calculated value of $g$ just equals to 0, the corresponding $v$ is the critical flutter velocity $v_{\mathrm{F}}$ of the wing. However, the flutter velocity obtained by this method is conservative.

## 2.2 Calculation results

### 2.2.1 Calculation verification

A large number of fluid elastic experiments and simulations on the control surfaces of ships and underwater vehicles have been done in the US navy David Taylor towing tank, and a lot of experimental data have been accumulated. According to the linear flutter calculation method in section 2.1, with the parameters in Reference [11], the corresponding relations of $v-g$ are calculated when the distances $x_a$ from the mass center to the elastic shaft in group A and group B are different, as shown in Fig. 2. Compared with the calculation results in the reference, the two are consistent with each other, which suggests that the linear flutter calculation method used in this paper is correct and Theodorsen theory can be

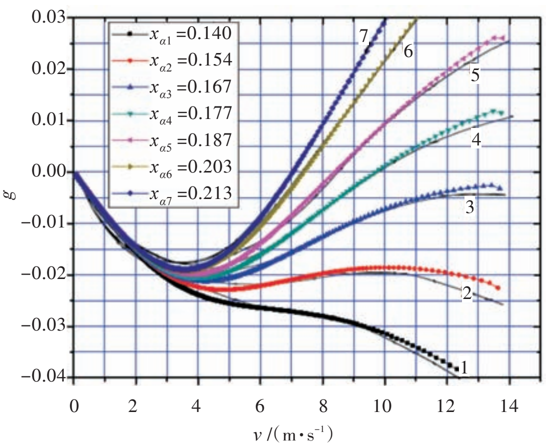


(a) Comparison between the simulation result in group A and calculation result in group A in reference

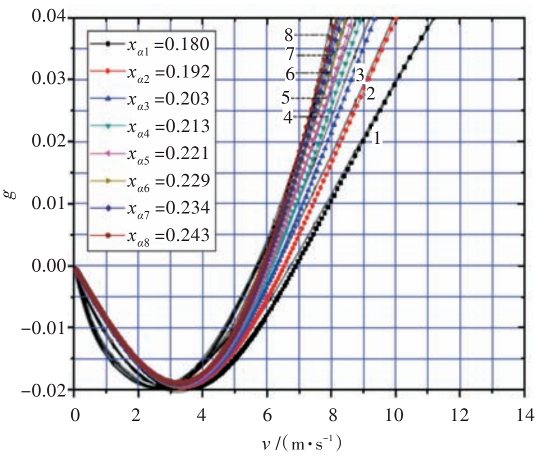


(b) Comparison between the simulation result in group B and calculation result in group B in reference

Fig.2 Calculation results of linear flutter in comparison with that of Reference [11] effectively used for the fluid elasticity simulation. As for the error in comparison, the main reason is the difference in model processing after analysis.

### 2.2.2 Calculation results and analysis of the influences of linear parameters on the flutter of rudder system

After correctness of the flutter calculation method above being verified, impacts of the linear parameters such as the frequency ratio $R_\omega$ and the mass ratio $\mu$ in the rudder system on flutters are calculated and analyzed.

With binary linear flutter model employed in the rudder system, Fig. 3 shows the use of $v-g$ method to calculate the impact trend of part of the linear parameters on $v_F$. The dimensionless turning radius of rudder blade to the stiffness center $r_a = 0.583$; $\mu = 2$; and $a = -0.48$. When the frequency ratio $R_\omega \approx 1$, $v_F$ is close to be the minimum; if the natural torsional frequency $\omega_\alpha$ of the system is increased while $R_\omega$ kept unchanged, $v_F$ will increase in direct proportion to $\omega_\alpha$; when $R_\omega < 1$, if $\omega_\alpha$ is increased singly, $v_F$ value will increase accordingly; if the natural heaving frequency $\omega_h$ of the system is increased, $v_F$ will decrease when $R_\omega < 1$. It can be seen that the main mode of flutter under this combination of parameters is torsional mode, that is, the torsion branch becomes unstable first. Therefore, increasing the torsional rigidity can greatly increase the $v_F$ value. In addition, antedisplacement of the dimensionless quantity $x_a$ of the mass center relative to the elastic shaft can increase the $v_F$ value, and the mass center can be advanced by increasing the balance weight at the leading edge of the wing.

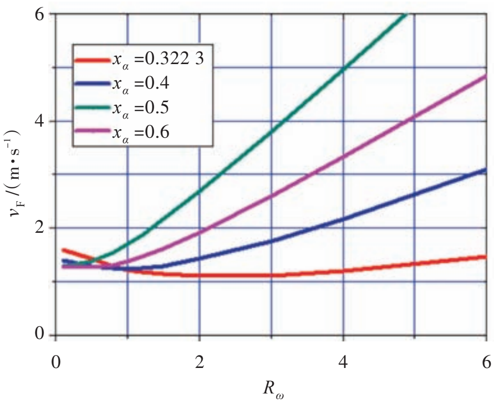


Fig.3 Influence of frequency ratio $R_\omega$ and $x_\alpha$ on flutter velocity

Fig. 4 shows the impact trend of mass ratio $\mu$ on $v_F$ under different $x_a$, where $r_a = 0.583$; $R_\omega = 0.549\,9$; and $a = -0.48$. In the figure, each curve has a minimum value $\mu_m$. In a specific structure, the mass $m$ and $\omega_\alpha$ do not change. When $\mu \leqslant \mu_m$, $v_F$ increases with a very large slope when $\mu \to 0$, which indicates that there is no danger of flutter when the rudder moves in high density medium; when $\mu > \mu_m$, low density medium will increase $v_F$, which is opposite to the result obtained when $\mu \leqslant \mu_m$.

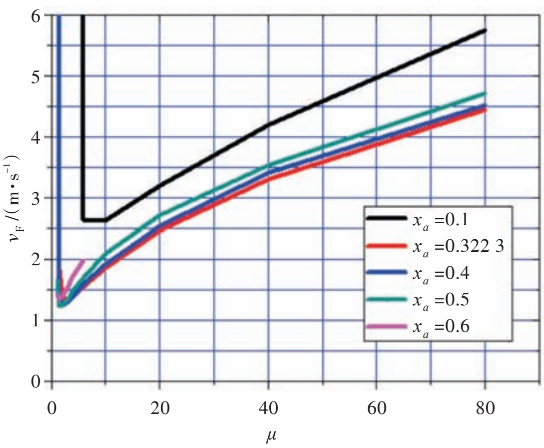


Fig.4 Influence of mass ratio $\mu$ on flutter velocity

## 3 Calculation and analysis of nonlinear flutters of binary wing

### 3.1 Calculation model

The motion differential equations of the lift and moment of the wing's arbitrary motion as well as the motion differential equation of nonlinear flutter of the binary wing are:

$$L = \pi\rho_a b^2\left[\ddot{h} + v\dot{\alpha} - b\bar{a}\ddot{\alpha}\right] + 2\pi\rho_a vb\left(Q_{3/4}(0)\phi_\omega\left(\hat{\tau}\right) + \int_0^{\hat{\tau}} \frac{dQ_{3/4}(\sigma)}{d\sigma}\phi_\omega\left(\hat{\tau} - \sigma\right)d\sigma\right) \tag{8}$$

$$T_\alpha = \pi\rho_a b^2 \cdot \left(b\bar{a}\ddot{h} - vb\left(\frac{1}{2} - \bar{a}\right)\dot{\alpha} - b^2\left(\frac{1}{8} + \bar{a}^2\right)\ddot{\alpha}\right) + 2\pi\rho_a vb^2\left(\bar{a} + \frac{1}{2}\right) \left(Q_{3/4}(0)\phi_\omega\left(\hat{\tau}\right) + \int_0^{\hat{\tau}} \frac{dQ_{3/4}(\sigma)}{d\sigma}\phi_\omega\left(\hat{\tau} - \sigma\right)d\sigma\right) \tag{9}$$

$$m\ddot{h} + mx_a\ddot{\alpha} + c_h\dot{h} + F(h) = -L(t) \tag{10}$$

$$mx_a\ddot{h} + m\gamma_a^{\,2}\ddot{\alpha} + c_\alpha\dot{\alpha} + G(\alpha) = T_\alpha(t) \tag{11}$$

where $Q_{3/4}$ is the downwash of the wing section's 3/4 chord point; $\phi_\omega\left(\hat{\tau}\right)$ is Wanger function; $c_h$ and $c_\alpha$ are the heaving and pitching damping coefficients of the wing section, respectively; $F(h)$ is the interval nonlinearity in the spring force; $G(\alpha)$ is the interval nonlinearity of the torsional spring's torque.

$F(h)$ and $G(\alpha)$ are the functions of $h$ and $\alpha$, respectively, and the curves are shown in Fig. 5, where $h_s$ is displacement interval and $\alpha_s$ is the angle interval. Specific expressions are shown in Eq. (12) and Eq. (13).

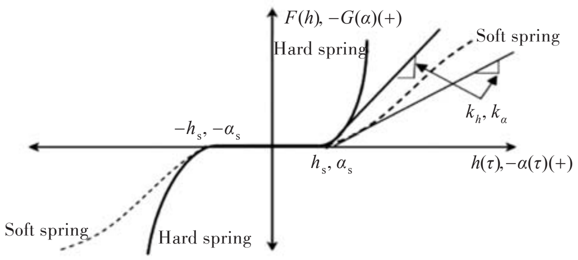


Fig.5 Schematic of interval nonlinearity

$$F(h)=\begin{cases} k_h(h-h_s)+\hat{k}_h(h-h_s)^3, & h>h_s \\ 0, & -h_s \leqslant h \leqslant h_s \\ k_h(h+h_s)+\hat{k}_h(h+h_s)^3, & h<-h_s \end{cases} \quad (12)$$

$$G(\alpha)=\begin{cases} k_\alpha(\alpha-\alpha_s)+\hat{k}_\alpha(\alpha-\alpha_s)^3, & \alpha>\alpha_s \\ 0, & -\alpha_s \leqslant \alpha \leqslant \alpha_s \\ k_\alpha(\alpha+\alpha_s)+\hat{k}_\alpha(\alpha+\alpha_s)^3, & \alpha<-\alpha_s \end{cases} \quad (13)$$

After the introduction of dimensionless parameters, the parameters can be rewritten as:

$$\begin{cases} \xi=h/b,\ \omega_\xi=\sqrt{k_h/m},\ \omega_\alpha=\sqrt{k_\alpha/(m\gamma_\alpha{}^2)}, \\ \bar{\omega}=\omega_\xi/\omega_\alpha,\ \ \bar{\gamma}_a=\gamma_a/b,\ \bar{x}_a=x_a/b, \\ \zeta_\xi=c_h/(2\sqrt{mk_h}),\ \zeta_\alpha=c_\alpha/(2\sqrt{m\gamma_a{}^2\cdot k_\alpha}) \\ R_\xi=\hat{k}_h b^2/k_h,\ R_\alpha=\hat{k}_\alpha/k_\alpha,\ \mu=m/(\pi\rho_\alpha b^2), \\ v_{\mathrm{non}}=v/(\omega_\alpha b),\ \bar{\tau}=vt/b \end{cases} \quad (14)$$

Let

$$\xi_s=\frac{h_s}{b},\ \ \eta_\alpha=\frac{\alpha_s}{\alpha} \quad (15)$$

where $\omega_\xi$ and $\omega_\alpha$ are the natural frequencies of coupling-free heaving and pitching, respectively; $\bar{\omega}$ is the frequency ratio; $\bar{x}_a$ is the dimensionless distance from the mass center of the wing to the elastic shaft; $\zeta_\xi$ and $\zeta_\alpha$ are damping ratios of the heaving and pitching movements, respectively; $v_{\mathrm{non}}$ is the dimensionless inflow velocity; $\bar{\tau}$ is the dimensionless time; $R_\xi$ is the dimensionless quantity of nonlinear heaving stiffness coefficient; $R_\alpha$ is the dimensionless quantity of nonlinear pitching stiffness coefficient; $\xi_s$ is the dimensionless quantity of the heaving interval; $\eta_\alpha$ is the dimensionless quantity of the pitching interval.

The following new state variables are introduced:

$$\begin{cases} \omega_1(\hat{\tau})=\int_0^{\hat{\tau}} \mathrm{e}^{-b_1(\hat{\tau}-\sigma)}\alpha(\sigma)\mathrm{d}\sigma \\ \omega_2(\hat{\tau})=\int_0^{\hat{\tau}} \mathrm{e}^{-b_2(\hat{\tau}-\sigma)}\alpha(\sigma)\mathrm{d}\sigma \\ \omega_3(\hat{\tau})=\int_0^{\hat{\tau}} \mathrm{e}^{-b_1(\hat{\tau}-\sigma)}\xi(\sigma)\mathrm{d}\sigma \\ \omega_4(\hat{\tau})=\int_0^{\hat{\tau}} \mathrm{e}^{-b_2(\hat{\tau}-\sigma)}\xi(\sigma)\mathrm{d}\sigma \end{cases} \quad (16)$$

So, Eq. (10)–Eq. (11) can be rewritten as follow:

$$c_0\ddot{\xi}+c_1\ddot{\alpha}+c_2\dot{\xi}+c_3\dot{\alpha}+c_4\eta_s+c_{44}\xi+c_5\alpha+c_6\omega_1+ c_7\omega_2+c_8\omega_3+c_9\omega_4+c_{10}\eta_s{}^3=\boldsymbol{f}(\hat{\tau}) \quad (17)$$

$$d_0\ddot{\xi}+d_1\ddot{\alpha}+d_2\dot{\xi}+d_3\dot{\alpha}+d_4\xi+d_5\eta_\alpha+d_{55}\alpha+d_6\omega_1+ d_7\omega_2+d_8\omega_3+d_9\omega_4+d_{10}\eta_\alpha{}^3=\boldsymbol{g}(\hat{\tau}) \quad (18)$$

where,

$$c_0=1+\frac{1}{\mu}$$

$$c_1=\bar{x}_a-\frac{\bar{a}}{\mu}$$

$$c_2=2\zeta_\zeta\frac{\bar{\omega}}{v_{\mathrm{non}}}+\frac{2}{\mu}(1-A_1-A_2)$$

$$c_3=\frac{1+2(0.5-\bar{a})(1-A_1-A_2)}{\mu}$$

$$c_4=\left(\frac{\bar{\omega}}{v_{\mathrm{non}}}\right)^2$$

$$c_{44}=\frac{2}{\mu}(A_1b_1+A_2b_2)$$

$$c_5=\frac{2}{\mu}[1-A_1-A_2]+(0.5-\bar{a})(A_1b_1+A_2b_2)$$

$$c_6=\frac{2}{\mu}A_1b_1[1-(0.5-\bar{a})b_1]$$

$$c_7=\frac{2}{\mu}A_2b_2[1-(0.5-\bar{a})b_2]$$

$$c_8=-\frac{2}{\mu}A_1b_1{}^2$$

$$c_9=-\frac{2}{\mu}A_2b_2{}^2$$

$$c_{10}=R_\xi\left(\frac{\bar{\omega}}{v_{\mathrm{non}}}\right)^2$$

$$d_0=\frac{\bar{x}_a}{\bar{\gamma}_a{}^2}-\frac{\bar{a}}{\mu\bar{\gamma}_a{}^2}$$

$$d_1=1+\frac{1+8\bar{a}^2}{8\mu\bar{\gamma}_a{}^2}$$

$$d_2=-\frac{(1+2\bar{a})(1-A_1-A_2)}{\mu\bar{\gamma}_a{}^2}$$

$$d_3=2\zeta_\alpha\frac{1}{v_{\mathrm{non}}}+\frac{1-2\bar{a}}{2\mu\bar{\gamma}_a{}^2}-\frac{(1-2\bar{a})(1+2\bar{a})(1-A_1-A_2)}{2\mu\bar{\gamma}_a{}^2}$$

$$d_4=\frac{(1+2\bar{a})(A_1b_1+A_2b_2)}{\mu\bar{\gamma}_a{}^2}$$

$$d_5 = \frac{1}{{v_{\text{non}}}^2}$$

$$d_{55} = -\frac{(1+2\bar{a})(1-A_1-A_2)}{\mu{\bar{\gamma}_a}^2} - \frac{(1-2\bar{a})(1+2\bar{a})(A_1 b_1 + A_2 b_2)}{2\mu{\bar{\gamma}_a}^2}$$

$$d_9 = -\frac{(1+2\bar{a})A_2{b_2}^2}{\mu{\bar{\gamma}_a}^2}$$

$$d_{10} = R_\alpha \frac{1}{{v_{\text{non}}}^2}$$

The $\boldsymbol{f}\left(\hat{\tau}\right)$ and $\boldsymbol{g}\left(\hat{\tau}\right)$ at the right sides of Eq. (17) and Eq. (18) are respectively:

$$\boldsymbol{f}\left(\hat{\tau}\right) = \frac{2}{\mu}[(0.5-\bar{a})\alpha(0) + \xi(0)] \cdot \left(A_1 b_1 \mathrm{e}^{-b_1\hat{\tau}} + A_2 b_2 \mathrm{e}^{-b_2\hat{\tau}}\right) \tag{19}$$

$$\boldsymbol{g}\left(\hat{\tau}\right) = \frac{1+2\bar{a}}{2{\bar{\gamma}_a}^2}\boldsymbol{f}\left(\hat{\tau}\right) \tag{20}$$

Eq. (8) - Eq. (11) of fluid elasticity are written in the following matrix form:

$$\boldsymbol{M}\ddot{q}\left(\hat{\tau}\right) + \boldsymbol{D}\dot{q}\left(\hat{\tau}\right) + \boldsymbol{Kq}\left(\hat{\tau}\right) + \boldsymbol{KKq}_\eta\left(\hat{\tau}\right) + \boldsymbol{F}\left(\boldsymbol{q}_\eta\left(\hat{\tau}\right)\right) + \boldsymbol{G\omega}\left(\hat{\tau}\right) = \boldsymbol{f}\left(\hat{\tau}\right) \tag{21}$$

where

$$\boldsymbol{M} = \begin{bmatrix} c_0 & c_1 \\ d_0 & d_1 \end{bmatrix};\quad \boldsymbol{D} = \begin{bmatrix} c_2 & c_3 \\ d_2 & d_3 \end{bmatrix};\quad \boldsymbol{K} = \begin{bmatrix} c_{44} & c_5 \\ d_4 & d_{55} \end{bmatrix}$$

$$\boldsymbol{KK} = \begin{bmatrix} c_4 & 0 \\ 0 & d_5 \end{bmatrix};\quad \boldsymbol{G} = \begin{bmatrix} c_6 & c_7 & c_8 & c_9 \\ d_6 & d_7 & d_8 & d_9 \end{bmatrix}$$

$$\boldsymbol{f}\left(\hat{\tau}\right) = \begin{bmatrix} f\left(\hat{\tau}\right) \\ g\left(\hat{\tau}\right) \end{bmatrix};\ \boldsymbol{q}\left(\hat{\tau}\right) = \begin{bmatrix} \xi\left(\hat{\tau}\right) \\ \alpha\left(\hat{\tau}\right) \end{bmatrix};\ \boldsymbol{q}_\eta\left(\hat{\tau}\right) = \begin{bmatrix} \eta_s\left(\hat{\tau}\right) \\ \eta_\alpha\left(\hat{\tau}\right) \end{bmatrix}$$

$$\boldsymbol{F}\left(\boldsymbol{q}_\eta\left(\hat{\tau}\right)\right) = \begin{bmatrix} c_{10}\left([1\quad 0]\boldsymbol{q}\left(\hat{\tau}\right)\right)^3 \\ d_{10}\left([1\quad 0]\boldsymbol{q}\left(\hat{\tau}\right)\right)^3 \end{bmatrix},$$

$$\boldsymbol{\omega}\left(\hat{\tau}\right) = \left\{\boldsymbol{\omega}_1\left(\hat{\tau}\right)\ \boldsymbol{\omega}_2\left(\hat{\tau}\right)\ \boldsymbol{\omega}_3\left(\hat{\tau}\right)\ \boldsymbol{\omega}_4\left(\hat{\tau}\right)\right\}^{\mathrm{T}}$$

Using the derivative Eq. (22) containing parametric variable integrals, the state vector $\boldsymbol{\omega}\left(\hat{\tau}\right)$ is found to satisfy differential Eq. (23).

$$\begin{cases} F(y) = \int_{x_1(y)}^{x_2(y)} f(x,y)\mathrm{d}x \\ \mathrm{d}F(y)/\mathrm{d}y = \int_{x_1(y)}^{x_2(y)} fy(x,y)\mathrm{d}x + f(x_2(y),y) \cdot \mathrm{d}x_2(y)/\mathrm{d}y - f(x_1(y),y)\mathrm{d}x_1(y)/\mathrm{d}y \end{cases} \tag{22}$$

$$\boldsymbol{\omega}'\left(\hat{\tau}\right) = \boldsymbol{E}_\omega\boldsymbol{\omega}\left(\hat{\tau}\right) + \boldsymbol{E}_q\boldsymbol{q}\left(\hat{\tau}\right) \tag{23}$$

where

$$\boldsymbol{E}_\omega = \begin{bmatrix} -b_1 & 0 & 0 & 0 \\ 0 & -b_2 & 0 & 0 \\ 0 & 0 & -b_1 & 0 \\ 0 & 0 & 0 & -b_2 \end{bmatrix}$$

$$\boldsymbol{E}_q = \begin{bmatrix} 0 & 1 \\ 0 & 1 \\ 1 & 0 \\ 1 & 0 \end{bmatrix}$$

According to Eq. (22) and Eq. (23), the dimensionless fluid elasticity equation of the two degrees of freedom binary nonlinear wing in the state space can be obtained and illustrated as follow:

$$\begin{Bmatrix} \dot{\boldsymbol{q}}\left(\hat{\tau}\right) \\ \ddot{\boldsymbol{q}}\left(\hat{\tau}\right) \\ \dot{\boldsymbol{\omega}}\left(\hat{\tau}\right) \end{Bmatrix} = \begin{bmatrix} 0_{2\times 2} & I_{2\times 2} & 0_{2\times 2} \\ -\boldsymbol{M}^{-1}\boldsymbol{K} & -\boldsymbol{M}^{-1}\boldsymbol{D} & -\boldsymbol{M}^{-1}\boldsymbol{G} \\ \boldsymbol{E}_q & 0_{4\times 2} & \boldsymbol{E}_\omega \end{bmatrix} \begin{Bmatrix} \boldsymbol{q}\left(\hat{\tau}\right) \\ \dot{\boldsymbol{q}}\left(\hat{\tau}\right) \\ \boldsymbol{\omega}\left(\hat{\tau}\right) \end{Bmatrix} + \begin{Bmatrix} 0_{2\times 1} \\ -\boldsymbol{M}^{-1}\boldsymbol{F}\left(\boldsymbol{q}_\eta\left(\hat{\tau}\right)\right) - \boldsymbol{M}^{-1}\boldsymbol{KKq}_\eta\left(\hat{\tau}\right) \\ 0_{4\times 1} \end{Bmatrix} + \begin{Bmatrix} 0_{2\times 1} \\ -\boldsymbol{M}^{-1}\boldsymbol{f}\left(\hat{\tau}\right) \\ 0_{4\times 1} \end{Bmatrix} \tag{24}$$

## 3.2 Calculation and analysis

Fig. 6 shows the response of fluid elasticity in the case that the heaving interval $\xi_s = 0.005$ and the pitching interval $\eta_\alpha = 0$. It can be seen from the figure that self-excited vibration with an equal amplitude occurs, that is, limit cycle oscillation. The existence of interval leads to a certain degree of freedom in the system difficult to control, and excites water noise, therefore, controlling interval and other nonlinear links are also essential to the control of wing vibration.

# 4 Conclusions

In this paper, the flutter law of linear rudder system is calculated and analyzed based on a binary wing linear flutter model, whose results are in agreement with the experimental data in Reference [11]. The nonlinear flutter phenomenon of the rudder system with interval is simulated and calculated by the hydrodynamic calculation method for two degrees of freedom binary wing in arbitrary time domain. The calculation results show that the smaller the distance from the mass center to the elastic shaft is, the more the flutter velocity is improved, and adding balance weight to the rudder blade is usually used to advance the mass center. The smaller the value of dimension-

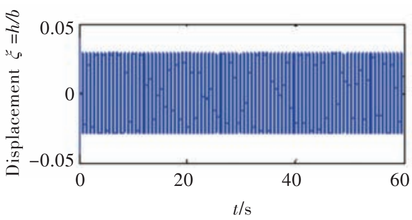

(a) Displacement variation as a function of time

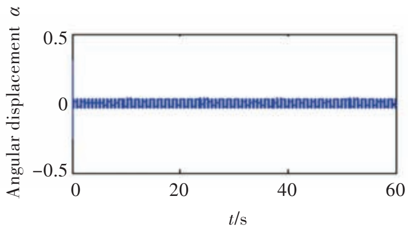

(b) Angular displacement variation as a function of time

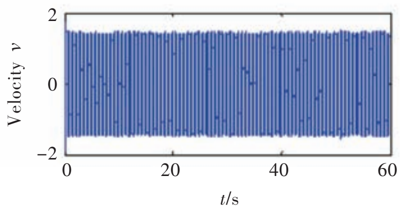

(c) Velocity variation as a function of time

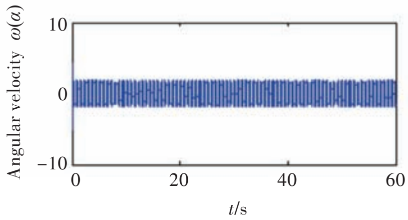

(d) Angular velocity variation as a function of time

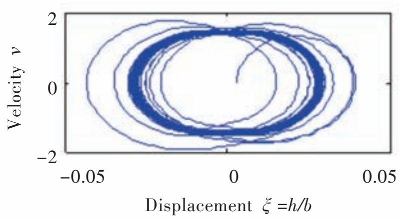

(e) Velocity variation as a function of displacement

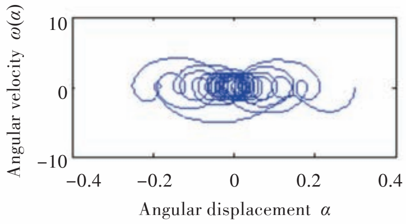

(f) Angular velocity variation as a function of angular displacement

Fig.6 Calculation results of interval nonlinearity

less density is, the more difficult it is for flutters to occur, that is, reducing the mass of the rudder blade is conducive to improve the flutter velocity. At the same time, it is also found that increasing the torsional rigidity of the rudder shaft has the same effect. Because of the nonlinear parameters in actual rudder system, such as interval and friction, the nonlinear simulation and calculation of interval in the system are needed. The existence of interval may result in the un-damped vibration response in the system, that is, limit cycle oscillation, which does not cause damage to the rudder blade structure, but will stimulate the water noise and other problems. In conclusion, it is of great significance to simulate and analyze the flutter of rudder system comprehensively. The analysis of the flutter of rudder system in this paper can provide basic research methods and references for this kind of simulation.

## References

[1] FORSCHING H W. 气动弹性力学原理[M]. SHEN Keyang, translated. Shanghai: Shanghai Scientific and Technological Literature Press, 1982(in Chinese).

[2] THEODORSEN T. General theory of aerodynamic instability and the mechanism of flutter: TR-496 [R]. [S.l.] : National Advisory Committee for Aeronautics (NACA), 1935.

[3] THEODORSEN T, GARRICK I E. Mechanism of flutter: a theoretical and experimental investigation of the flutter problem TR-685 [R]. [S.l.]: National Advisory Committee for Aeronautics(NACA), 1938.

[4] DOWELL E H, CURTIS H C, Jr, SISTO F. A modern course in aeroelasticity[M]. CHEN Wenjun, YIN Chuanjia, translated. Beijing: China Aerospace Press, 1991(in Chinese).

[5] WRIGHT J R, COOPER J E. Introduction to aircraft aeroelasticity and loads[M]. New York: John Wiley & Sons Ltd, 2008.

[6] CHU Yiqing, LI Cuiying. 非线性振动分析[M]. Beijing: Beijing Institute of Technology Press, 1996 (in Chinese).

[7] TSIEN H S.The Poincare-lighthill-kuo method[J]. Advan Appl Mechan, 1956,4: 281-349.

[8] LIM C W, WU B S. A new analytical approach to the Duffing-harmonic oscillator [J].Phys Lett: A, 2003, 311(4/5): 365-373.

[9] LV Hexiang, ZHU Jufen, MA Liying. Discussion of analysing of geometric non-linear beams with large rotations[J].Chinese Journal of Computational Mechanics, 1995, 12(4): 485-490(in Chinese).

[10] YIN Youquan. 非线性有限元基础[M]. Beijing: Peking University Press, 2007(in Chinese).

[11] JEWELL D A, MCCORMICK M E. Hydroelastic instability of a control surface: DTMB-TR-1442 [R]. Carderok, MD: David Taylor Model Basin, 1961.

# 舵系统的颤振计算与分析

肖清[1]，谢俊超[1]，陈东阳[2]
1 中国舰船研究设计中心，湖北 武汉 430064
2 南京理工大学 发射动力学研究所，江苏 南京 210094

**摘　要：**为了研究舵系统水弹性特性，基于二元水翼线性颤振模型对舵系统的颤振特性进行数值计算与分析，计算结果与文献仿真数据较为吻合，验证了模型的有效性。利用该模型计算和分析频率比、重心、扭转刚度等线性参数对舵系统颤振的影响规律。此外，结合两自由度二元水翼任意运动时域水动力计算方法，对舵系统非线性颤振现象进行计算，获取传动间隙等因素对非线性颤振的影响规律。研究结果表明：减小质心到弹性轴的距离、增加舵的扭转刚度，有利于提高颤振速度；间隙等非线性因素的存在可能导致系统出现极限循环振荡，激发噪声，应加以控制。

**关键词：**舵系统；水弹性；颤振；间隙；非线性

[*Continued from page* 15]

# 维修工具使用的可达域计算及可视化方法

方雄兵[1]，田正东[2]，林锐[1]，李涛涛[1]
1 中国舰船研究设计中心，湖北 武汉 430064
2 海军装备部，北京 100841

**摘　要：**针对开展虚拟维修时相关仿真软件缺乏维修工具使用时的可达性分析功能之问题，提出一种可达域计算方法以及可达域的三维可视化方法。首先，根据虚拟人手臂结构特点，计算出虚拟人手臂尺寸；在此基础上，结合工具的外沿点位置，给出工具使用时的最远可达距离计算方法；基于该距离值及虚拟人手臂长度值计算可达域几何体放大尺度，利用该尺度可以对工具使用时的可达域进行三维可视化。最后，结合Jack仿真软件，Tcl/Tk以及Python语言，实现了维修工具使用可达性的分析功能。仿真实例表明：所实现的方法能满足工具使用时的可达性分析，所提供的仿真报告自动生成功能有助于仿真人员编制报告。

**关键词：**维修工具；可达性分析；可达域；图形可视化；Jack仿真软件